

日本原子力研究開発機構機関リポジトリ
Japan Atomic Energy Agency Institutional Repository

Title	Estimating fission-barrier height by the spherical-basis method
Author(s)	Hiroyuki Koura
Citation	Progress of Theoretical and Experimental Physics, 2014(11), 113D02
Text Version	Publisher
URL	http://jolissrch-inter.tokai-sc.jaea.go.jp/search/servlet/search?5043735
DOI	http://dx.doi.org/10.1093/ptep/ptu148
Right	Originally published in Progress of Theoretical and Experimental Physics, 2014, 11, 113D02 © The Author(s) 2014. Published by Oxford University Press on behalf of the Physical Society of Japan.

Estimating fission-barrier height by the spherical-basis method

Hiroyuki Koura*

Advanced Science Research Center, Japan Atomic Energy Agency, 2-4 Shiakata-shirane, Tokai-mura, Naka-gun, Ibaraki 319-1195, Japan

*E-mail: koura.hiroyuki@jaea.go.jp

Received October 24, 2013; Revised September 4, 2014; Accepted September 29, 2014; Published November 1, 2014

.....
A novel method of estimating fission-barrier heights is presented in this paper, in which potential energy surfaces are calculated by using the spherical-basis method. This method is based on the idea of configuration mixing of various spherical states for deformed nuclei, which gave the ground-state nuclear-mass calculation presented by our group [H. Koura, T. Tachibana, M. Uno, and M. Yamada, Prog. Theor. Phys., **113**, 305 (2005)]. Under the restriction of symmetric fission, a systematical fission-barrier calculation is performed in the heavy and superheavy nuclear-mass region, and some higher (neighboring ^{252}Fm , known) and lower (neighboring ^{278}Ds , unknown) fission-barrier regions are found in the nuclear-mass chart; the origin of these appearances is discussed in the framework of the spherical-basis method. The calculated nuclei are also located in the unknown neutron-deficient superheavy nuclear-mass region, where nuclear fission determines a limit on the existence of nuclei. Three regions that have relatively high fission barriers are predicted in neutron-deficient regions having neutron numbers of around 126, 184, and 228.
.....

Subject Index D12

1. Introduction

In the region of heavy and superheavy nuclei, various decay modes coexist, such as α -decay, β -decay, and spontaneous fission. Spontaneous fission is a dynamical and drastic decay process in which a nucleus splits into two (sometimes three or more) nuclei. This mechanism is part of the nuclear many-body problem and is rather complicated. Nuclear fission is, of course, important due to its providing a large amount of atomic energy. In addition, nuclear fission is the main reason for the instability of heavy nuclei due to the Coulomb repulsive force, more than α -decay. Understanding the fission mechanism therefore leads to an understanding of the limit on the existence of nuclei with a high- Z (proton) number.

Bohr and Wheeler [1] qualitatively described the mechanism of nuclear fission by using the liquid-drop model. Later, Strutinsky developed a method of calculating shell-correction energies by using deformed single-particle levels [2,3]. The method of using deformed single-particle potentials to obtain deformed shell energies [4,5] is often referred to as the Nilsson–Strutinsky method. We note that nuclear energy can thus be regarded as having two components: macroscopic liquid-drop energy and microscopic shell energy. The idea of calculating the fission barrier from the deformed single-particle configuration and the liquid-drop energy was elaborately extended to the macroscopic–microscopic calculation by Möller and his collaborators. They presented several versions of their model, e.g., the finite-range droplet model (FRDM) [6] and the finite-range liquid-drop model (FRLDM) [7].

In contrast, other calculations for the fission barrier have been carried out based on a microscopic approach using Skyrme-type effective interactions [8,9]. We will not describe this approach here in detail; however, we point out for discussion in this paper that it is based on a consideration of a deformed single-particle configuration with a coordinate constraint in order to obtain fission barriers, in which a nucleus is well deformed.

In the above-mentioned calculations, a nuclear shape (or a constraint) is assumed and set in advance, and then a search is made for the eigenstate for its shape. In this paper, we propose a novel method of calculating a fission barrier that uses an approach that is radically different from using deformed single-particle states. We establish “spherical” single-particle states of the difference number of nucleons for one nucleus, and a deformed nuclear state is regarded as a representation of a configuration mixing of each of the spherical single-particle states. If the prepared spherical states yield a complete set in the quantum system, this assumption has validity in quantum mechanics.

Several years ago, we developed a method of calculating ground-state nuclear masses for the entire region of a nuclear chart; these are the KUTY and KTUY mass formulae [10], which we also refer to as the spherical-basis method. In contrast to other methods, we do not use deformed single-particle states; instead, we express the deformed nuclear states as configuration mixtures of various spherical single-particle states (some corrections are introduced). We successfully described the ground-state shell energies of deformed nuclei; the calculated ground-state masses accurately reproduced those that were experimentally measured, and the derivatives of the masses as neutron and proton separation energies were better than those calculated by other models available at that time. The deformation parameters were also obtained, and they were comparable to experimentally measured nuclear deformations [11].

In this paper, we apply the spherical-basis method for calculating the heights of fission barriers. Compared with a ground-state nuclear-mass calculation, a fission-barrier calculation requires larger deformations. Using this method, we give the fission-barrier landscape in the heavier nuclear-mass chart, and discuss the origin of the appearance of nuclei with significantly higher and lower fission barriers than those of surrounding nuclei. Furthermore, we use the fission-barrier heights to estimate a border indicating the existence of nuclei.

The mass asymmetry and large deformation are essentially important factors in discussing the fission phenomenon. In order to focus on their qualitative properties, however, nuclear shapes are limited to being axially and reflectionally symmetric, and only small deformations are considered in this paper. A discussion on the fission-fragment mass distribution cannot be given in this work due to this lack of asymmetric shape. This extension to asymmetric deformations will be left as a task for future work.

The rest of this paper is organized as follows. In Sect. 2, we give a short explanation of the method. The results and discussion are presented in Sect. 3, and our conclusions are presented in Sect. 4.

2. Method

The spherical-basis method [10] is based on the assumption that a deformed state of a nucleus can be regarded as a superposition of “spherical states” that correspond to concentric spheres with different radii. Under this assumption, the nuclear shell energy with deformations can be expressed as weighted sums of spherical shell energies, and the weights are obtained from geometric shapes. The spherical shell energy of a nucleus for a given proton number, Z , and for a neutron number, N , are obtained by totaling the single-particle levels, subtracting the averaged bulk energy, and by making adjustment for pairing effects, such as the Bardeen–Cooper–Schrieffer (BCS) configuration, and the

highly excited state components. The spherical shell energies of a nucleus with Z and N are defined for neutrons and protons, and are denoted as $E_{\text{nsh}}^{\text{sp}}(Z, N)$ and $E_{\text{psh}}^{\text{sp}}(Z, N)$.

This summation and extraction is analogous to the Strutinsky method [2,3], except for the treatment of the deformation and the deduction of the bulk energy. We are able to compute the spherical shell energies of any nuclei by using the global spherical single-particle potential [14].

Suppose a nucleus is deformed into, e.g., a rugby-ball shape. In this case, the nucleus has both minimum and maximum radii from the center to the surface. Each of these radii can be assigned to a spherical nucleus with the same radius. Under this consideration, we assume that a deformed nucleus can be decomposed into a part of a spherical nuclei with various radii, and the shell energy can be expressed as a part of the spherical shell energy with a certain weight. We describe the relation between a radius and the number of protons Z' or neutrons N' in the spherical nucleus. We adopt $r(Z') = (Z'/Z)^{1/3} R_0$ or $r(N') = (N'/N)^{1/3} R_0$ with $R_0 = 1.2A^{1/3}$ fm as the relation. The shell energy of a deformed nucleus with proton number Z and neutron number N is obtained as a weighted sum of the spherical shell energies and the macroscopic liquid-drop deformation energy as

$$E_{\text{sh}}(Z, N, \text{def.}) = \sum_{Z'} W_{\text{p}}(Z'; Z, N) E_{\text{psh}}^{\text{sp}}(Z', N'') + \sum_{N'} W_{\text{n}}(N'; Z, N) E_{\text{nsh}}^{\text{sp}}(Z'', N') \\ + \Delta E_{\text{surf}}(Z, N, \text{def.}) - \Delta E_{\text{Coul}}(Z, N, \text{def.}) - \Delta E_{\text{pro}}(Z, N, \text{def.}). \quad (1)$$

Here, N'' and Z'' are the integers closest to $Z' \cdot N/Z$ and $N' \cdot Z/N$, respectively. This means that a charge equilibrium in a nucleus is assumed in this calculation. The meaning of the spherical proton and neutron shell energies, $E_{i\text{sh}}^{\text{sp}}$ ($i = \text{p, n}$), was explained earlier, and W_i ($i = \text{p, n}$) are their mixing weights. The weight W_i is expressed by using the solid angle $\Omega(r)$ for a given distance r from the center as

$$W_{\text{p}} = -\frac{1}{4\pi} \frac{d\Omega(r(Z'))}{dZ'}. \\ W_{\text{n}} = -\frac{1}{4\pi} \frac{d\Omega(r(N'))}{dN'}. \quad (2)$$

The weight depends on nuclear shapes through the solid angle.

The quantities ΔE_{surf} and ΔE_{Coul} in Eq. (1) are the differences due to deformation of the macroscopic surface and the Coulomb energies. Other corrections are explained in Ref. [10]. The ground-state shell energy is obtained by minimizing the sum in Eq. (1) with respect to the deformation, denoted by “def.”, and the results are shown in Refs. [10].

In this paper, we focus on larger deformations in which there are various saddle points, the highest of which can be regarded as a fission saddle, or fission barrier.

In our previous work on calculating ground-state masses, it was necessary to determine spherical shell energies for nuclei with proton numbers of up to 270 and neutron numbers of up to 400, which correspond to the higher excited states caused by deformations in the model space; these are shown in Fig. 2 of Ref. [10]. This is sufficient if we only consider ground-state masses for nuclei with proton numbers ranging up to 130 and neutron numbers up to 200. However, in the case of fission barriers, we found by performing the preliminary calculations that many more spherical shell energies are necessary [12,13]. Thus, we extended these calculations to include spherical shell energies for proton numbers of up to 670 and neutron numbers of up to 998. The procedure for calculating the spherical shell energies is the same as that in Ref. [10].

We limited the deformations of nuclei to only those with axial and reflectional symmetry, parametrized by α_2 , α_4 , and α_6 , as in the ground-state mass calculations [10]. The radius is then

expressed as

$$R(\theta) = \frac{R_0}{\lambda} [1 + \alpha_2 P_2(\cos \theta) + \alpha_4 P_4(\cos \theta) + \alpha_6 P_6(\cos \theta)], \quad (3)$$

where λ is introduced to guarantee volume conservation and is defined as

$$\lambda = \left[1 + \frac{3}{4\pi} \left(\frac{4\pi}{5} \alpha_2^2 + \frac{4\pi}{9} \alpha_4^2 + \frac{4\pi}{13} \alpha_6^2 \right) \right]^{1/3}. \quad (4)$$

In order to analyze just the qualitative properties, we expand the liquid-drop parts ΔE_{surf} and ΔE_{Coul} in terms of the deformation parameters ($\alpha_{2,4,6}$, including the cross terms) and use the terms up to the fourth order. This reduces computational time by omitting the four-dimensional numerical integrals of the Coulomb energy. If we compare this fourth-order approximation with the full calculations for a few selected nuclei, we see that it is accurate to within a deformation of $\alpha_2 \leq 0.4$ – 0.5 . We thus focus primarily on $\alpha_2 < 0.4$.

We would like to emphasize that these parameter values are not changed or optimized for the fission-barrier height: they are the ones that best reproduced the experimental ground-state masses, as presented in the initial paper [10].

Finding a saddle point in multiparameter space is essentially difficult; see, e.g., Ref. [7]. Thus, we simply performed a 2D saddle-point search; i.e., we first calculated the shell energy with various values of α_2 and α_4 , with $\alpha_6 = 0$, then we found the minimum with respect to α_6 . Next, we searched for a saddle point by looking for a location at which there was both positive and negative curvature in each set of orthogonal coordinates. After the search, we inspected selected cases to ascertain the validity of the search method, and we found no unreasonable results. We used a mesh size of 0.01 for α_2 and α_4 , and 0.001 for α_6 . For the ground-state mass, a more accurate search for the minimum was carried out.

3. Results and discussion

3.1. Comparison of experimental and calculated fission-barrier heights

Figure 1 shows a comparison between the experimental fission-barrier heights [15] and the heights calculated using models for radium and actinide isotopes ($Z = 88$ – 96). In the case of the experimental barrier heights, both the inner and outer barriers are indicated if they are experimentally identified. The experimental barrier heights [15] lie in the range of 4–9 MeV. Our estimated barrier heights generally matched the higher barrier from among the inner and outer experimental barriers, like Np, Pu, Am, and Cm. In the case of the Th, Pa, and U regions, however, the heights were overestimated by ~ 1 MeV. From the experimental data in Ref. [15], the shapes of the outer barrier for known isotopes from Th to Cm are known as mass asymmetry. In this paper, we only perform calculations for symmetric shapes, and thus we cannot make a comparison among barriers in the Th, Pa, and U regions because the shapes of these barriers appear to be asymmetric. We note that the outer fission barrier would be lower if we included an additional degree of freedom for asymmetry. If we adopt the higher barrier from among the inner and outer barriers as an experimental barrier for comparison with the calculated ones, the RMS deviation from the experimental barrier for the 52 adopted nuclei is 0.71 MeV, and the average difference from the experimental value is +0.37 MeV. For the extended Thomas–Fermi plus Strutinsky integral (ETFSI) [9], which is based on the Strutinsky approach with a two-body interaction as the Skyrme-type effective force, we adopted a β_2 , β_4 , and β_6 parametrization for the nuclear shape, which is essentially the same parametrization used in this study. The ETFSI fission barriers well reproduce the experimental trends, including those in

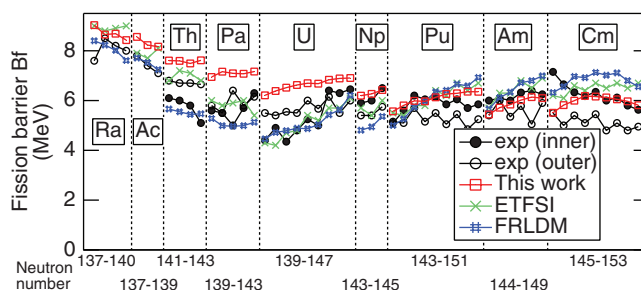


Fig. 1. Comparison between calculated and experimental fission-barrier heights. Circle: experiment [15]; open circle represents outer barrier, filled circle represents inner barrier. Square: this study. Cross: ETFSI [9]. Hash mark: FRLDM [7]. In the theoretical values, only the highest fission barriers are plotted because only the highest barriers appeared in the original papers [7,9].

the Th, Pa, and U regions. The RMS deviation for the same nuclei is 0.61 MeV, and the average difference from the experimental value is +0.05 MeV. We also plotted the FRLDM [7], which is the latest version of the macroscopic–microscopic approach and which uses 5D parametrization that includes a parameter for asymmetry. The RMS deviation is 0.77 MeV, and the average differences is -0.19 MeV.

3.2. Landscape of fission-barrier height

Figure 2 shows the fission-barrier heights for symmetric shapes in the heavy and superheavy nuclear-mass region ranging from 76 to 148 of Z , and from 120 to 270 of N . Known nuclei are indicated by small black squares. In the known nuclear region, there is a kind of “hill” around $Z \approx 100$ and $N \approx 150$. The fission barrier in this region is about 6 MeV and it is higher than those of neighboring nuclei. This region includes actinide nuclei with measured fission-barrier heights as shown in Fig. 1. Another “basin” region is also found around $Z \approx 110$ and $N \approx 168$. The heights of these nuclei are generally lower than those of neighboring nuclei, and are in the range of 1–3 MeV. These nuclei are expected to be fissioning nuclei due to their lower fission barriers. Actually, spontaneously fissioning nuclei [16,17] were found experimentally, shown as open squares in Fig. 2, which, as expected, are in the same region.

Similar results are found for the ETFSI method, as shown in Fig. 3. The regions of higher (“hill”) and lower (“basin”) barriers are also seen, although the location of the “basin” is shifted to the neutron-richer side and is away from the experimentally fissioning region. Note that the fission barriers of the ETFSI method are calculated from deformed single-particle levels.

In order to clarify the origin of the significantly higher and lower barriers than those of surrounding nuclei in our method, as shown in Fig. 2, we show two cases: ^{252}Fm ($Z = 100$, $N = 152$) as a case of a “hill” region, and ^{278}Ds ($Z = 110$, $N = 168$) as a case of a “basin” region. Figure 4 (upper) shows the potential energy surface of ^{252}Fm . The deformation parameters at the saddle point are $\alpha_2 = 0.27$, $\alpha_4 = 0.03$, and $\alpha_6 = 0.01$. Generally, the neutron and proton numbers of a well deformed nucleus are far from the number of a closed-shell number, or a magic number. In the spherical-basis method, if a nucleus is deformed, the weighted sum of the spherical shell energies decreases, while the sum of the macroscopic deformed liquid-drop energy increases. An explanation of the lowering of the energy due to the weighted sum is given as follows. Figure 5 shows the mixing weight in this deformation and corresponding spherical shell energies in the case of a saddle-point shape. In such a well deformed shape, minimum and maximum radii exist, and the corresponding numbers of

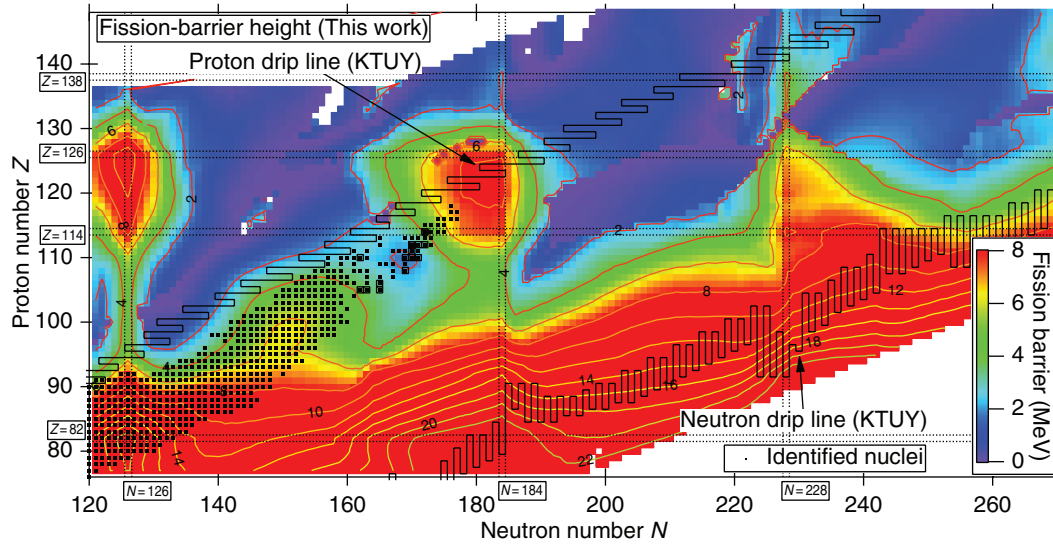


Fig. 2. Fission-barrier height in the heavy and superheavy mass region. Proton and neutron drip lines from the KTUY mass formula are shown as solid lines. Known nuclides [16,17] are also shown, as small black squares. Nuclei for which fission events were measured as occurring at a rate of 10% or more are shown as open squares (only for nuclei with neutron numbers $N > 161$). These are in the region $Z \approx 110$ and $N \approx 168$, as shown in the figure.

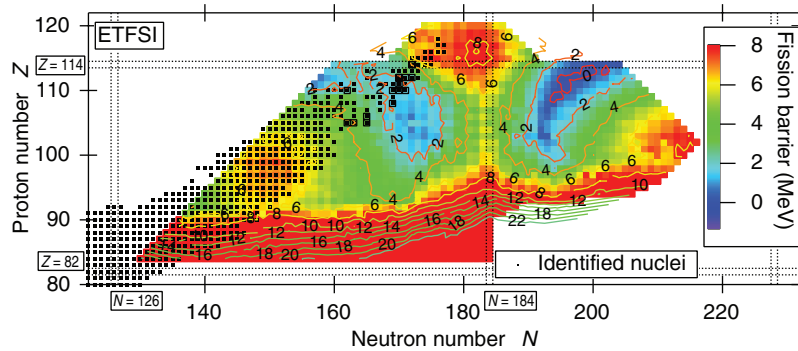


Fig. 3. Fission-barrier heights estimated by ETFSI [9].

neutrons and protons are also defined. In the case of neutrons, 97 is the corresponding number of neutrons to the minimum radius, and 232 is the corresponding number to the maximum radius. The summation is conducted through this range. In the case of protons, 64 and 152 are the smallest and largest numbers of protons. In Fig. 5, the end of the left side is the minimum number, and the end of the right side is the maximum number. Of these four numbers of nucleons, only 232 for neutrons is the closest number to the closed shell, 228. The weighted sum of spherical shell energies lowers the total energy, and the appearance of the saddle in this case comes from the 228 neutron shell closure. The other three sides of the weight (fewer neutrons and both more and fewer protons) do not reach strong shell closures, and thus do not lower the saddle point. The energy is therefore not lowered by much: ~ 6 MeV.

Figure 4 (lower panel) shows the potential energy surface of ^{278}Ds . The deformation parameters are $\alpha_2 = 0.18$, $\alpha_4 = -0.01$, and $\alpha_6 = 0.007$. The mixing weight and spherical shell energies of ^{268}Ds at the saddle point are shown in Fig. 6. In this case, the smaller side of the neutron weight reaches the $N' = 126$ neutron shell closure, and also the smaller side of the proton weight reaches the $Z' = 82$

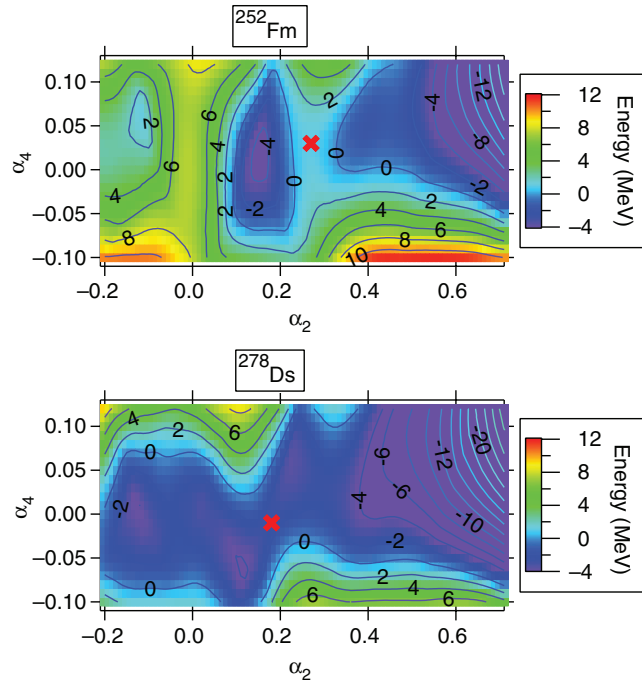


Fig. 4. Potential energy surface. Minimization by α_6 has been carried out. The highest saddle point is indicated by a cross. Upper: ^{252}Fm . Lower: ^{278}Ds .

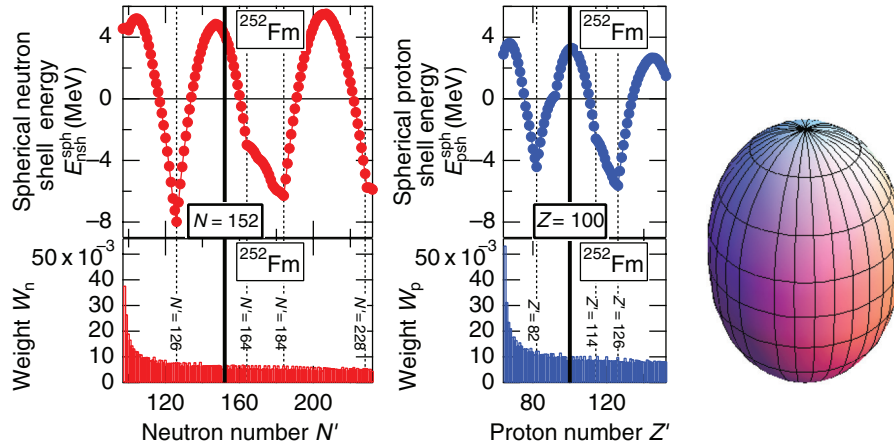


Fig. 5. (Left) Mixing weights (lower) and corresponding spherical shell energies (upper) at the saddle point for ^{252}Fm . Each quantity appears in Eq. (1). (Right) Shape at the saddle point for ^{252}Fm .

proton shell closure. These two regions of weights produce the minimum of the saddle, and furthermore the weights in the smaller particle region (or inner nuclear region) have large values, as shown in the figures. In other words, this configuration can be regarded as a component of the core of ^{208}Pb ($Z = 82$ and $N = 126$) plus (collective) valence nucleons. Thus, this configuration has a saddle point with much lower values: 1–3 MeV in this mass region.

3.3. Limit of existence of nuclei from systematics of fission-barrier heights

Again going back to Fig. 2, we can see some isolated “islands” in the neutron-deficient heavy and superheavy mass region. The island in the lighter-mass region is found along $N = 126$ with $Z \approx 114$

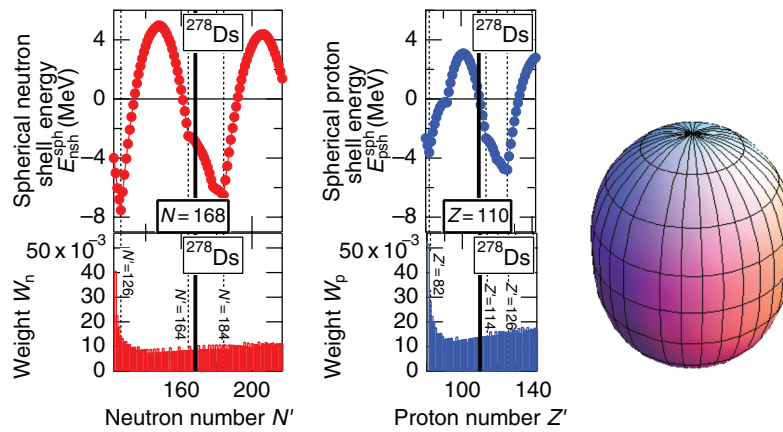


Fig. 6. (Left) Mixing weights and corresponding spherical shell energies at the saddle point for ^{278}Ds . (Right) Shape at the saddle point for ^{278}Ds . See explanation in Fig. 5.

and 126. This island is caused as a result of the strong shell closure of $N = 126$ and $Z = 114$ and 126, and the barrier heights of these nuclei are more than 8 MeV. However, the existence of nuclei in this region is unexpected because this region is far outside the proton drip line. Because of the existence of this island, the fission barriers of the neutron-deficient nuclei near $N \sim 126$ are enhanced, compared to the macroscopic estimation, and some nuclei such as U and Pu isotopes would be expected to have longer half-lives, and have more heavy-ion synthesis cross sections due to an enhancement of the evaporation-residue cross section.

The island along $N = 184$ with Z between approximately 114 and 126 is expected to be an island of stability in the superheavy mass region. The estimated barrier height is more than 8 MeV. The adopted nuclear potential in this work results in doubly magic spherical single-particle levels for ^{298}Fl ($Z = 114$) and $^{310}[126]$ [18]. The proton shell gaps of 114 for ^{298}Fl and 126 for $^{310}[126]$ are comparable (actually the gap of 126 is slightly larger than that of 114), and this property results in the creation of an island.

In the much heavier region, a peninsula appeared along $N = 228$ with Z between 114 and 126. This enhanced region is due to the strong shell gap of $N = 228$, and the reason the well defined island disappeared is that the nucleus $^{354}[126]$ is not a doubly magic nucleus in this nuclear potential (see Ref. [18]). Nevertheless, the barrier height of this nucleus is obtained as 6.59 MeV, comparable with those of the known actinides, as shown in Fig. 1, and α_2 at the saddle point is 0.12. Furthermore, this nucleus is estimated to be β -stable [18]. Therefore, we can expect that this nucleus has a comparatively long half-life.

3.4. Borders of the inner and outer fission barriers

Figure 7 shows the deformation parameter α_2 at the saddle point. In the known actinide region ($90 < Z < 103$ and $120 < N < 160$), there is a distinct border of $\alpha_2 \approx 0.4$. As we move from the border in the direction of higher Z , the saddle-point α_2 deformation is approximately 0.2–0.3, and the highest saddle point is the inner one if the outer barrier exists. As we move toward lower Z , the saddle-point α_2 deformation is more than 0.4, and the highest saddle point is the outer one if the inner barrier exists. If we compare these to the experimentally determined locations of such transitions, as shown in Fig. 1, we see that the calculated location of the transition is shifted to a region in which Z includes one or two more protons. Our calculations reproduced the qualitative trend of the

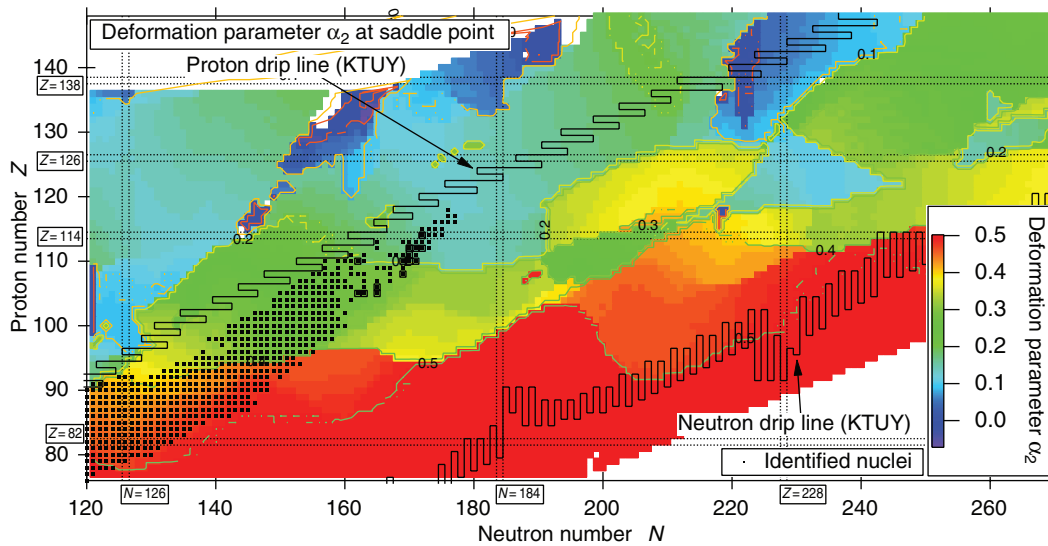


Fig. 7. α_2 deformation parameter at the fission saddle point. See explanation in Fig. 2.

experimentally determined locations of the dominant outer and inner barriers. For a more quantitative analysis, however, it will be necessary to extend our method to include larger deformations and asymmetric shapes.

4. Conclusion

We have presented a novel method for estimating the heights of fission barriers. We used the spherical-basis method instead of the Nilsson–Strutinsky framework to explain the existence of basins and hills in the superheavy mass region. In this study, however, we limited the nuclear shape to small deformations so that we could focus on the reasons for the shape of the landscape. An important area of our future work will be to apply this method to asymmetric shapes as, thus far, we have only considered shapes with axial and reflectional symmetry, but in general, especially with larger deformations, nuclear shapes are asymmetric. Recently, we have begun some calculations of potential energy surfaces for shapes with axial symmetry but without reflectional symmetry, for some selected nuclei in the same framework [19]. We will next extend our method to asymmetric shapes.

Acknowledgements

We wish to thank Prof. M. Yamada and Prof. S. Chiba for their valuable discussions. This work was partly supported by Grant-in-Aid for Young Scientists (B) 19740151, provided by the Ministry of Education, Culture, Sports, Science and Technology (MEXT) of JAPAN. The numerical calculations were mainly carried out using the PRIMERGY BX900 computer at the Center for Computational Science and E-Systems, Japan Atomic Energy Agency.

References

- [1] N. Bohr and J. A. Wheeler, *Phys. Rev.*, **56**, 426 (1939).
- [2] V. M. Strutinsky, *Nucl. Phys. A*, **95**, 420 (1967).
- [3] V. M. Strutinsky, *Nucl. Phys. A*, **122**, 1 (1968).
- [4] S. G. Nilsson, *Dan. Mat. Fys. Medd.*, **29**, 16 (1955).
- [5] S. G. Nilsson et al., *Nucl. Phys. A*, **131**, 1 (1969).
- [6] P. Möller, J. R. Nix, W. D. Myers, and W. J. Swiatecki, *At. Data Nucl. Data Tables*, **59**, 185 (1995).

- [7] P. Möller, A. J. Sierk, T. Ichikawa, A. Iwamoto, R. Bengtsson, H. Uhrenholt, and S. Åberg, *Phys. Rev. C*, **79**, 64304 (2009).
- [8] A. Mamdouh, J. M. Pearson, M. Rayet, and F. Tondeur, *Nucl. Phys. A*, **644**, 389 (1999).
- [9] A. Mamdouh, J. M. Pearson, M. Rayet, and F. Tondeur, *Nucl. Phys. A*, **679**, 337 (2001).
- [10] H. Koura, M. Uno, M. Uno, and M. Yamada, *Nucl. Phys. A*, **674**, 47 (2000).
- [11] S. Raman, C. W. Nestor Jr, and P. Tikkanen, *At. Data Nucl. Data Tables*, **78**, 1 (2001).
- [12] H. Koura, *AIP Conf. Proc.*, **561**, 388 (2001).
- [13] H. Koura, *J. Nucl. Radiochem. Sci.*, **3**, 201 (2002).
- [14] H. Koura and M. Yamada, *Nucl. Phys. A*, **671**, 96 (2000).
- [15] T. Belgia et al., *Handbook for Calculations of Nuclear Reaction Data* (IAEA, Vienna, 2006), RIPL-2, IAEA = TECDOC-1506.
- [16] T. Tachibana, H. Koura, and J. Katakura, *Chart of the Nuclides 2010 (Japanese Nuclear Data Committee and Nuclear Data Center)* (Japan Atomic Energy Agency, Tokai, Ibaraki, 2010).
- [17] Yu. Ts. Oganessian et al., *Phys. Rev. Lett.*, **109**, 162501 (2012).
- [18] H. Koura and S. Chiba, *J. Phys. Soc. Jpn.*, **82**, 14201 (2013).
- [19] H. Koura, Meeting Abstract of the Phys. Soc. Jpn. **68**, 51 (2013) [in Japanese].